Available online at www.sciencedirect.com

ScienceDirect

Procedia CIRP 58 (2017) 529 – 534

www.elsevier.com/locate/procedia

16th CIRP Conference on Modelling of Machining Operations

Discrete elements model of an abrasive water-jet through the focal canon to the work-piece

Romain Laniel[a,*], Otman Bouchareb[a], Antoine Brient[a], Mathieu Miroir[a]

[a] *IPR, UMR 6251, 263 Av. Gal. Leclerc, 35042 Rennes, France*

* Corresponding author. Tel.: +33-223-234-088; fax: +33-223-236-111. *E-mail address:* romain.laniel@univ-rennes1.fr

Abstract

Abrasive water-jet manufacturing process can shape a lot of materials ranging from metals to glasses. It has a lot of advantages, as its low cutting forces, but remains quite difficult to control. Indeed, the process is leaded by the abrasive particle trajectories which depends on the water static pressure and many other parameters. The impact pressure on the work-piece is commonly modeled by a two Gaussian fit sum which are representative of the particles velocity distribution and the granulometry respectively. Today no studies based on discrete elements take into account the mixing chamber and the focal canon which are the two main steps of the abrasive water-jet tool constitution. In this preliminary work we propose to model the flow through the focal canon until the target impact by an original numeric granular approach. The Non-Smooth Contact Dynamics is an efficient method on a large range of simulation domains. In our case, we consider the water phase and the abrasive phase as two collections of distinct polydisperse elements. The masses are corrected and the contact interaction laws are adjusted to account for an equivalent fluid which similar mechanical properties. These two phases are mixed in a chamber and focalised through the canon, knowing water static pressure and abrasive mass rate. After the canon end the abrasive water-jet evolves in air and thus decelerates by friction. The tool-fluid adapts its geometric configuration from this kinetic energy decrease and impacts a target plane located at a known distance from the canon. Such a model is built on some classic process parameters as the water static pressure, the abrasive mass rate or the work-piece vs. canon distance, but it also naturally takes into account finer mechanical parameters as the abrasive granulometry or friction dissipation. Simulations gives interesting results of impact pressure distribution on the target work- piece with dynamic data of all the collection particles. More generally, this work final aim is to link elemental particle damage studies with a macroscopic wear prediction law.

Peer-review under responsibility of the scientific committee of The 16th CIRP Conference on Modelling of Machining Operations

Keywords: Abrasive Water-Jet, Discrete Element Model

1. Industrial context: the AWJ non-through machining

Abrasive water-jet manufacturing process, also known as AWJ process, is used to achieved cutting of various materials by means of a high-pressure water-jet mixed with abrasive grains [1]. The water-jet flows from a pump to a cutting head where abrasive grains can be added in a mixing chamber before the AWJ is expelled through the focal canon, cf. Fig. 1. If AWJ can cut samples with a thickness of several tens of millimeters, it can also and paradoxically, achieve pocket milling by defining appropriate machining parameters that would allow the material not to be pierced through. One of the advantages of waterjet machining, the lack of thermal distortion on the work-piece, as well as the machining versatility of this process has lead to investigate the industrial feasibility of metallic work-pieces AWJ milling [2,3]. The manufacturing strategy as well as the cutting head speed are obviously key parameters to achieve pocketing [4] but many other parameters, as declination angle [5], abrasive mass flow rate, pressure, feeding direction, also influence the quality of the surface finish, especially studied for alluminium cutting [6]. AWJ is also widely used for brittle materials [7] cutting however AWJ pocketing of glass has not yet been achieved industrially. Brittleness of glass brings challenging issues when material removal process is involved, e.g. grinding [8]. Smooth surface finish, in particular, is hard to obtained since material removal would induce surface damages as well as sub-surface damages. Being able to shape a glass work-piece with the versatility of a 5-axis cutter would bring innovative prospects for glass industry. The evolution of the roughness and waviness according to transverse speed have been studied in [9]. When traverse speed increases, material volumes of peaks and core roughness as well as void volumes of valleys and core roughness tend to decrease. Interestingly, the decrease of these four parameters is very similar, and the ratio between material and void stays roughly the same. Overall this shows that the surface waviness amplitude decreases with transverse speed while keeping its “craters and mounts” aspect. It is

Peer-review under responsibility of the scientific committee of The 16th CIRP Conference on Modelling of Machining Operations
doi:10.1016/j.procir.2017.03.267

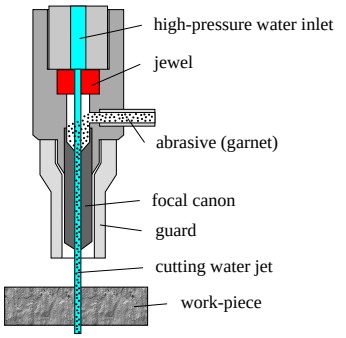

Fig. 1. Schematic drawing of the AWJ process.

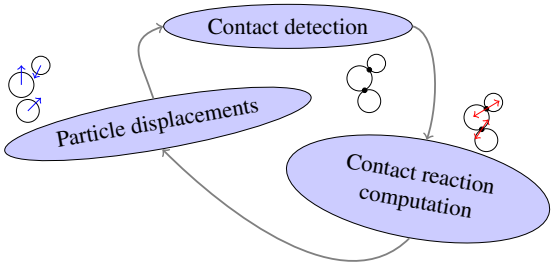

Fig. 2. Algorithm pattern of a single iteration of discrete element method.

characterized by several damage scales. At roughness scale, cracks, peaks and core roughness tend to increase in the same proportions when transverse speed increases. At waviness scale the increase of transverse speed limits the material removal and therefore the amplitude of the waviness. The material and void volume ratio remains the same despite the waviness amplitude decrease. This preliminary study of AWJ pocketing of glass has enlightened two damage scales. The roughness scale involved by elementary abrasive impact and the waviness scale involved by the complex trajectory of the AWJ tool-fluid on the work-piece wear surface. In both cases, the knowledge of the AWJ tool-fluid constitution and kinetic distribution is a necessary preliminary condition before predicting and optimizing the glass surface finish of such a process. Several finite elements models propose to analyze the impact of water [10] or a single abrasive particle [11] or a little collection of abrasive particles [12,13] on specific materials, as PMMA, steel and titanium alloys respectively. Unfortunately, the finite element approach limits the number of modeled abrasive particles [14]. *A contrario*, the multiphasic fluid approach [15,16] gives interesting results about the tool-fluid distributions, but does not give the local impact mechanisms. In this study, a discrete elements method is applied to model the AWJ. This approach, built on contact mechanics, is used to simulate the behaviour of the tool-fluid through the focal canon to the work-piece. It is well known that the AWJ velocity field decreases and evolves after the canon expel. The proposed model has to take into account this dissipation phenomena. In the framework of AWJ non-through machining, the material removal depth are often related to the pressure distribution on the free surface of the target piece [17]. Such a model allows to link the energetic and pressure distributions.

2. A Non Smooth Contact Dynamics model applied to AWJ

2.1. The discrete model introduction

Simulation methods of fluid *vs.* particles interaction problems have been proposed in [18,19]. Nevertheless, the first method is computational costly and both of them are very little adapted to determine the entire contact network of large multi-contact problems, cf. Fig. 2. In this study background we propose to use the non smooth contact dynamics theory a.k.a NSCD [20,21]. This method is able to solve multi-contact problems with the expression of dynamics equations in the α-contact local frame. Such transformations are achieved by the $\boldsymbol{H}_\alpha$ operator and $\boldsymbol{H}_\alpha^T$ operator which transport velocities and forces from the particle frame to the α-contact frame and *vice versa*. For an integration time step $i+1$ a linear relation is found between the relative velocity v_{i+1}^α and the average impulsion p_{i+1}^α on the interval $[t_i, t_{i+1}]$. This one is associated with an interaction law such as,

$$\begin{cases} v_{i+1}^\alpha - \boldsymbol{W}^{\alpha\alpha} p_{i+1}^\alpha = v_{\text{free},i}^\alpha + \sum_{\beta\neq\alpha} \boldsymbol{W}^{\alpha\beta} p_{i+1}^\beta \\ \text{Law}[v_{i+1}^\alpha, p_{i+1}^\alpha] = \text{true} \ . \end{cases} \tag{1}$$

External forces F_{ext} and dynamics effects are taken into account by the relative velocity free of contacts $v_{\text{free},i}^\alpha$ and the Delassus operator $\boldsymbol{W}^{\alpha\beta} = \boldsymbol{H}_\alpha^T \boldsymbol{M}^{-1} \boldsymbol{H}_\beta$ which appears naturally with $\boldsymbol{M}$ the mass matrix. Several types of interaction law can be used between two contactors. The most used interaction law for granular materials is a Signorini contact condition on the normal direction $0 \leq v_{n,i+1} \perp p_{n,i+1} \geq 0$ associated with a Coulomb friction law on the tangential direction. The multi-contact problem is solved implicitly by a Gauss-Seidel loop which goes through contacts, and stops when energetic and interpenetration criteria are satisfied.

2.2. The AWJ simulation

The discrete elements simulation of the AWJ process is carried out by the following steps:

- Definition of a quasi-dense granular sample with a controled granulometry similar to the abrasive particles one. The construction method used is based on geometric deposit of spherical particles [22].
- Deposit simulation under gravity of the granular sample inside the canon cylinder container limited by an horizontal plane. The final sample has a known volume.
- Random selection of abrasive particles to reach the targeted ratio of abrasive particle. The other particles are seen as water and their density is computed to offset the empty volume between beads. We notice that the granulometry of the selected abrasive particles is checked as the same as the initial one.

- Process simulation with initialization of particle velocities to a homogeneous field v_0. Particles are allowed to get out from the canon cylinder end and impact a target horizontal plane located to a vertical distance h.

To compare the sensitivity of these AWJ simulations, most of the numeric parameters are the same, especially the sample construction ones. In this study, the discrete sample is built with 7828 spherical particles of linear granulometry centered around $\varnothing$ 120 μm $\mp$ 10 %, which corresponds to a MESH 120. They are put inside the canon cylinder container of $\varnothing$ 1 mm diameter. The AWJ non-through machining on glasses needs a weak pressure around 30 MPa and a canon/work-piece distance ranging 10 – 15 mm. The initial value of velocity is chosen to reach the 30 MPa of water cinematic pressure $\rho_w \frac{v_0^2}{2} \Rightarrow v_0 \simeq 245$ m.s^{-1} with ρ_w the water specific mass. The distance h is arbitrary chosen to 10 mm and the abrasive density is 4000 kg.m^{-3}, close to the garnet one, which is the most used abrasive material.
The behaviour of the tool-fluid modeled by a collection of rigid bodies depends also on the contact parameters as the energy restitution and the friction. To assure that this discrete model give good agreement with the water phase, simulations of pure water jet impact are carried out with a various range of contact parameters. Comparisons are made between the reference reaction on the target plane $F_{ref} = \rho_w S_{wj} v_0^2$, with S_{wj} the impact surface of the water jet, and the average reaction $\overline{F}$ extracted from the discrete simulations. In Fig. 3 we see that the energy restitution and the friction disturb the water jet. For the future simulations, we consider soft and frictionless contacts for the "water beads".

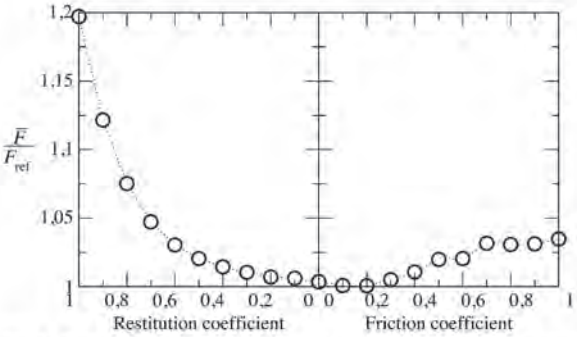

Fig. 3. Relative evolution of the AWJ reaction on plane according to contact parameters: energy restitution and friction coefficient.

The tool-fluid breaking effect is simplified as a determination problem of air effects on the beads [23]. In fact, in a first approximation, we consider a two distinct velocity domains with an homogeneous v_0 field before the canon limit and a null field after the canon limit. This induces aerodynamic forces on the granular medium after the canon end. Thanks to this approach, position of a rigid body j can be determined as a function, among other things, of external forces $F_{ext,j}$ of j body including aerodynamic contribution defined by the equation 2.

$$F_{ext,j} = m_j g + \underbrace{C\rho_a \pi r_j^2 \|(v_a(x_j) - v_j)\|(v_a(x_j) - v_j)}_{\text{Aerodynamic contribution}} \quad (2)$$

with v_a the air velocity field, x_j, v_j, r_j and m_j position, velocity, radius and mass of the particle j, g the gravity acceleration, ρ_a the air specific mass and $C \simeq 0,5$ the penetration coefficient of a sphere in fluid. This external force gives good agreement with a simple breaking model of a single sphere bead k, of mass m_k and projected surface S_k, thrown with initial velocity v_0 in a null air velocity field. The final velocity v_h after a fall distance h is given in equation 3.

$$v_h = v_0 e^{-\frac{h}{\lambda_k}}, \lambda_k = \frac{2m_k}{\rho_a C S_k} \quad (3)$$

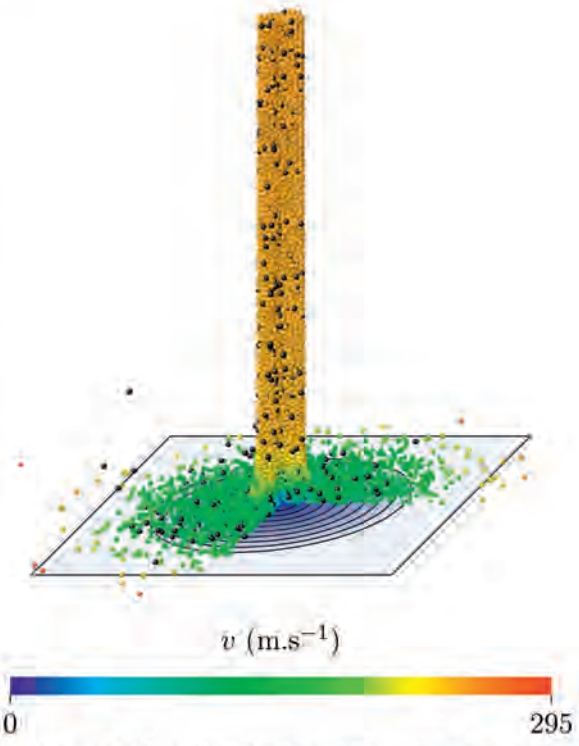

Fig. 4. Example of $\frac{3}{4}$ of AWJ granular medium and its velocity field simulated just after impact, with 10 mm of canon/work-piece distance and 5 % of volumic ratio of abrasive particles. These last ones are drawn in black.

In this simple model, the gravity is neglected because of the quite high particle velocities. The dense granular medium is not sensitive to external forces inside the canon, but once out of it, aerodynamic contributions decrease the particle velocities. This abrupt change involves an increment of radial forces in the contact network located at the canon end; this phenomenon ac-

celerates its erosion. The sample has been generated in a dense configuration, so every particle deviatoric movement is transmitted to its neighborhood. The energy dissipation thus modifies the distribution of all the sample which tend to gradually enlarge its diameter as the mass conservation principle should predict it.

2.3. First validation by pressure distribution

Once the simulation data are recorded, elementary contact reactions are easy to distinguish and to extract. However, the highly dynamic nature of the process causes a lot of noise. The mean reaction on all or part of the target plane area, as $\overline{F}$ for example, are averaged in a stabilized time range. The reactions are split into several concentric rings to catch the radial dependencies of the tool-fluid pressure, cf. Fig. 4 & 5. Let us recall that the three main models of AWJ erosion, Finnie [24], Bitter [25] and Hashish [26,27], all consider that wear power of an AWJ, normal to the target plane, is directly linked to the square of impact velocity which is proportional to the pressure. The shape of this pressure is often seen as a double Gaussian fit with respect to radius r, relative to the granulometry, the velocity field distribution and the abrasive distribution respectively [16]. In our case, the initial velocity is homogeneous, so the different ring pressures are fitted with a simple Gaussian $P(r)$ as described in equation 4.

$$P(r) = \underbrace{\frac{\overline{F}}{\pi r_G^2}}_{P_{max}} \mathrm{e}^{-\left(\frac{r}{r_G}\right)^2} \text{ with } \iint_{\infty} P(r)\mathrm{d}S = \overline{F} \qquad (4)$$

This fit depends only on the influence radius r_G, which is seen as the standard deviation, and is forced to give the global reaction $\overline{F}$ extracted from the simulations. Thus, the amplitude P_{max} is computed *a posteriori*. The Fig. 6 shows an example of the proposed post-treatment applied to a pure water-jet directly thrown to the target plane, i.e. $h = 0$.

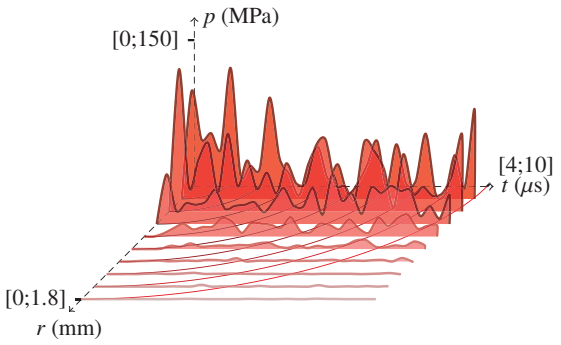

Fig. 5. Evolution of a pure water-jet pressure split on several concentric rings, according to time. This simulation does not take into account air dissipation phenomenon.

The ring pressures have to be considered carefully because of the granular nature of this model. It is well known that granular media react with particular contact network which form some arches. In this study, this involves a model artifact with a weak contact network in the center of the granular flow. For rings wide enough, this artifact does not appear but the consequence is that only too few ring pressures are representative. We chose to reduce the ring width and to exclude the first ring pressure from the Gaussian fit as illustrated in Fig. 6 by the red dot.

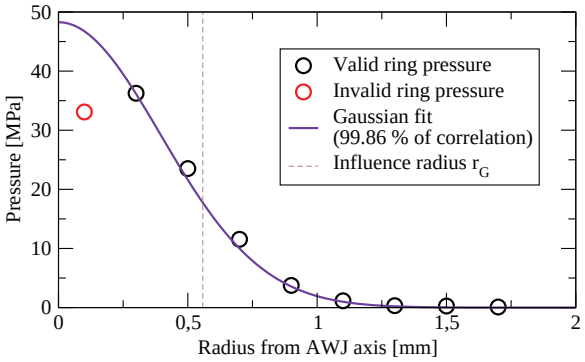

Fig. 6. Simulation values & Gaussian fit of a pure water-jet pressure split on several concentric rings, without air dissipation phenomenon.

3. Numerical simulation design & its representative results

In this study, the numerical granular model assumes an homogeneous field of velocity inside the focal canon, which is obviously non realistic. However, its interest is to investigate the energetic conditions applied to the work-piece according to the initial conditions and process parameters. We thus focus our comparisons on two specific parameters: the canon/work-piece height h which is representative of the dissipation and diffusion phenomena, and volume ratio of abrasive particles Cv_{ab} which is representative of the impact energy and the wear power. The numerical design is defined by (h, Cv_{ab}) and simulates the two distinct evolution of the tool-fluid: without abrasive particles and $h \in \{0, 3, 4, 5, 6, 7, 8, 9, 10\}$ mm, and with $Cv_{ab} \in \{1, 1.5, ..., 5\}$ % and $h = 10$ mm. The share test is obtained with the point (10 mm, 0 %). For each point a numeri-

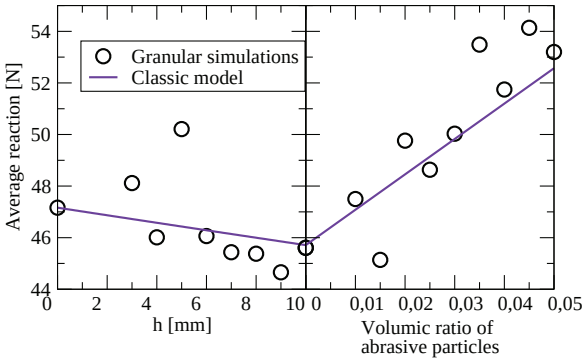

Fig. 7. Evolution of the AWJ reaction according to process parameters: canon/work-piece height h and volumic ratio of abrasive particles. Data from granular simulations are compared to the predictive model.

h [mm]	Cv_{ab} [%]	Correlation [%]	P_{max} [MPa]	r_G [mm]	$\overline{F}$ [N]
0	0	99.86	48.27	0.558	47.16
3	0	99.93	45.91	0.578	48.17
4	0	99.69	40.78	0.599	46.01
5	0	99.68	42.38	0.614	50.21
6	0	99.93	40.06	0.605	46.06
7	0	98.86	34.85	0.644	45.44
8	0	99.94	44.27	0.571	45.38
9	0	99.92	40.74	0.591	44.66
10	0	99.82	35.79	0.637	45.61
10	1	99.87	43.34	0.591	47.5
10	1.5	99.74	36.09	0.631	45.14
10	2	99.72	43.29	0.605	49.76
10	2.5	99.77	40	0.622	48.63
10	3	99.3	41.58	0.619	50.03
10	3.5	98.55	40.46	0.649	53.48
10	4	99.93	46.78	0.593	51.74
10	4.5	99.88	46.89	0.606	54.14
10	5	99.95	47.1	0.6	53.2

Table 1. Gaussian fit parameters: maximum pressure P_{max}, influence radius r_G and average reaction $\overline{F}$ with respect to both simulation parameters canon/work-piece height h and volumic ratio of abrasive particles Cv_{ab}.

cal simulation is carried out, a stabilized field of contact reaction is selected and the post-treatment described in the Sec. 2 is applied. The Gaussian fit parameters are extracted and complied in the Tab. 1. We notice that for all the simulation made, the minimum of correlation coefficient is 98.55 % which tends to prove the good fit of pressure by a simple Gaussian. Especially the pure water jet simulations, which give good agreement with the fit, show that without a random distribution of abrasive masses nor a velocity gradient in the focal canon, the pressure profile is still Gaussian thanks to the flow nature of the tool. This qualitative validation is a first step in building the discrete model of AWJ. Future simulations of the mixing mechanisms would allow to compare the numerical pressure distribution with experiments.

Moreover the reaction on the target plan globally decreases with the canon/work-piece height and globally increases with the volume ratio of abrasive particles. These tendencies are plotted in Fig. 7. The $F(h, Cv_{ab})$ predictive model used is based with the simple breaking model described in equation 3 and applied to the entire normal section of the AWJ in one hand, and the equivalent specific mass of the tool-fluid on the other hand. It is written as,

$$F(h, Cv_{ab}) = (Cv_{ab}\rho_{ab} + (1 - Cv_{ab})\rho_w)S_{wj}v_0^2 e^{-\frac{2h}{\overline{\lambda}}} \qquad (5)$$

with ρ_{ab} the density of abrasive material and $\overline{\lambda}$ the average of λ_k on the entire granular collection. Simulation data match with the predictive model of the equation 5, however some disturbances appear. They are caused by the dynamic nature of these approach with stabilized time range not long enough. This may be avoided with the repetition of simulation of different equivalent granular samples, which requires more computation time.

Finally, the Gaussian fits of this set of simulations allow to quantify the reorganization of the tool-fluid due to the air breaking effect. As mentioned in the Sec. 2, the AWJ enlarge as it decelerates during its fall. The influence radius r_G of the Gaussian

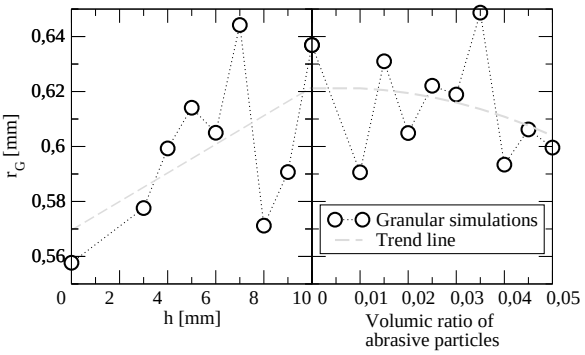

Fig. 8. Evolution of the Gaussian fit influence radius according to process parameters: canon/work-piece height h and volumic ratio of abrasive particles. These data are extracted from granular simulations and the trend lines are plotted.

fit catches this geometry modification as illustrated in Fig. 8. We have to notice that such a parameter is very sensitive to the extracted ring pressure, which are themselves very sensitive to the time range of averaging. Nevertheless, and despite some "numeric accidents", the good tendency is returned by the pure water simulations. Indeed, the mass conservation principle coupled with the equation 3 allow to write that the relative evolution of $r_G(h, 0)$ is equal to $e^{\frac{h}{2\overline{\lambda}}} - 1$. This is in good agreement with the trend line of the first part of the Fig. 8. More surprising, the increase of the volume ratio of abrasive particle tends to focal the AWJ. The abrasive particles, heavier than the water ones, are more difficult to deviate from their initial trajectory.

4. Conclusions & Prospects

A discrete approach of the simulation of an AWJ has been proposed. It involves specific process parameters as the granulometry and ratio of abrasive particles, the canon diameter, the canon/work-piece high, the wear angles, the traverse speed.

Input data is a collection of sphere particles relative to the tool-fluid and the initial velocity field. Non realistic assumptions have to be made on the distributions. Output data are all the state variables of the granular medium. In all cases, pressure profile can be extracted and fit by a simple Gaussian in the homogeneous initial velocity field framework. This first distribution depends only on the flow nature of the AWJ. A second Gaussian is usually observed in AWJ footprint on several materials and might be due to a specific distribution of velocity or abrasive particles. This difference is investigated in a work still in progress by simulating the mixing mechanisms in the mixing chamber. The discrete approach has allowed to define a predictive model of the energetic impact distribution with regards to the process parameters.

Future work will also focus on the work-piece final shape prediction by simulating the elementary mechanism of material removal. Also and since the abrasive quality modifies the wear efficiency [28] abrasive particles could be replaced by polyhedron to model more precisely the behaviour of AWJ.

References

[1] J. Folkes, *Waterjet — An innovative tool for manufacturing*, Journal of Materials Processing Technology 209, 6181–6189, 2009

[2] G.A Escobar-Palafox, R. Gault, K. Ridgway, *Characterisation of abrasive water-jet process for pocket milling in Inconel 718*, Vol. 1, 404-408, 2012

[3] G. Fowler, I. R. Pashby, P. H. Shipway, *Abrasive water-jet controlled depth milling of Ti6Al4V alloy – an investigation of the role of jet–workpiece traverse speed and abrasive grit size on the characteristics of the milled material*, Journal of Materials Processing Technology 161, 407–414, 2005

[4] M. C. Kong, D. Axinte, W. Voice, *An innovative method to perform maskless plain waterjet milling for pocket generation: a case study in Ti-based superalloys*, IJMTM 51, 642-648, 2011

[5] L. M. Hlaváč, I. M. Hlaváčová, L. Gembalová, J. Kaličinský, S. Fabian, J. Měšťánek, J. Kmec, V. Mádr, *Experimental method for the investigation of the abrasive water jet cutting quality*, Journal of Materials Processing Technology 209, 6190-6195, 2009

[6] S. Hloch, J. Valíček, *Topographical anomaly on surfaces created by abrasive waterjet*, Int J Adv Manuf Technol 59, 593–604, 2012

[7] C. Selvan, M. Raju, *Abrasive Waterjet Cutting Surfaces of Ceramics – An Experimental Investigation*, International Journal of Advanced Scientific Engineering and Technological Research 1(3), 52-59, 2012

[8] A. Brient, M. Brissot, T. Rouxel, J.-C. Sangleboeuf, *Influence of Grinding Parameters on Glass Workpieces Surface Finish Using Response Surface Methodology*, Journal of Manufacturing Science and Engineering. 133(4), 445011-445016, 2011

[9] A. Brient, R. Laniel, M. Miroir, G. Le Goic, S. Samper, J.-C. Sangleboeuf, *Multiscale Topography Analysis of Waterjet Pocketing of Silica Glass Surfaces*, Met. & Props., Charlotte (USA), March 2015

[10] C.-Y. Hsu, C.-C. Liang, T.-L. Teng, A.-T. Nguyen, *A numerical study on high-speed water jet impact*, Ocean Engineering 72, 98-106, 2013

[11] M. Junkar, B. Jurisevic, M. Fajdiga, M. Grah, *Finite element analysis of single-particle impact in abrasive water jet machining*, Int. Journal Impact Eng. 32(7), 1095-1112, 2006

[12] M. S. El Tobgy, E. Ng, M. A. Elbestawi, *Finite element modeling of erosion wear*, Int. J. of Machinig Tools and Manufacture 45(11), 1337-1346, 2005

[13] N. Kumar, M. Shukla, *Finite element analysis of multi-particle impact on erosion in abrasive water jet machining of titanium alloy*, J. Comp. App. Math. 236(18), 4600-4610, 2012

[14] S. Anwar, D. A. Axinte, A. A. Becker, *Finite element modelling of abrasive waterjet milled footprints*, J. of Materials Processing Technology 213(2), 180-193, 2013

[15] T. Mabrouki, K. Raissi, A. Cornier, *A numerical simulation and experimentatal study of the interaction between a pure high velocity waterjet and targets: contribution to investigate the decoating process*, Wear 239, 260–273, 2000

[16] M. Zaki, *Modélisation et simulation numérique du procédé de perçage non débouchant par jet d'eau abrasif*, PhD thesis, ENSAM, 2009

[17] D. S. Srinivasu, D. A. Axinte, P. H. Shipway, J. Folkes, *Influence of kinematic operating parameters on kerf geometry in abrasive waterjet machining of silicon carbide ceramics*, Int. J. Mach. Tools Manuf. 49(14), 1077-1088, 2009

[18] B.K. Cook, D.R. Noble, J.R. Williams. *A direct simulation method for particle-fluid system*, Engineering Computations, Vol. 21, 151-168, 2004.

[19] M.W. Schmeeckle, J.M. Nelson. *Direct numerical simulation of bedload transport using a local, dynamic boundary condition*, Sedimentology, Vol. 50, 279-301, 2003.

[20] M. Jean. *The non smooth contact dynamics method*, Comp. Meth. App. Mech. Eng., Vol. 177S, 235-257, 1999

[21] J.-J. Moreau. *Some numerical methods in multibody dynamics : application to granular material*, Eur. J. Mech. A Solids, Vol. 13, 93-114, 1994.

[22] R. Laniel, P. Alart, S. Pagano. *Discrete element investigations of wire-reinforced geomaterial in a three-dimensional modeling*, Computational Mechanics, Vol. 42, 67-76, 2008.

[23] R. Laniel, M. Tchikou, J.-C. Sangleboeuf, *A discrete elements simulation and analysis of a high energy stirred milling process*, Mech. and Ind. 13, 415-421, 2012

[24] I. Finnie, *Some reflections on the past and future of erosion*, Wear 186(1), 1-10, 1995

[25] J. A. Bitter, *A study of erosion phenomena*, Wear 6, 5-21 (part I), 169-190 (part II), 1963

[26] M. Hashish, *A model study of metal cutting with abrasive water jet*, ASME J. Engng. Mat. and Techn. 106, 88-100, 1984

[27] M. Hashish, *Optimization factors in abrasive waterjet machining*, Transaction of ASME J. Eng. Ind. 113, 29-37, 1991

[28] A. Khan, M. Haque, *Performance of different abrasive materials during abrasive water jet machining of glass*, Journal of Materials Processing Technology 191, 404–407, 2007